Available online at www.sciencedirect.com
ScienceDirect
Planetary and Space Science 55 (2007) 2164–2172
Planetary and Space Science
www.elsevier.com/locate/pss

Local plasma processes and enhanced electron densities in the lower ionosphere in magnetic cusp regions on Mars

E. Nielsen[a,*], M. Fraenz[a], H Zou[a], J.-S. Wang[a], D.A. Gurnett[b], D.L. Kirchner[b], D.D. Morgan[b], R. Huff[b], A. Safaeinili[c], J.J. Plaut[c], G Picardi[d], J.D. Winningham[e], R.A. Frahm[e], R. Lundin[f]

[a]*Max Planck Institute for Solar System Research, 37191 Katlenburg-Lindau, Germany*
[b]*Department of Physics and Astronomy, University of Iowa, Iowa City, IA 52242, USA*
[c]*Jet Propulsion Laboratory, Pasadena, CA 91109, USA*
[d]*Infocom Department, "La Sapienza", University of Rome, 00184 Rome, Italy*
[e]*Southeast Research Institute, P.O. Drawer 28510, San Antonio, TX 78228-0510, USA*
[f]*Swedish Institute of Space Physics, Box 812, S-98128 Kiruna, Sweden*

Received 24 January 2007; received in revised form 3 July 2007; accepted 6 July 2007
Available online 26 July 2007

Abstract

Both the MARSIS ionospheric sounder and the charged particle instrument package ASPERA-3 are experiments on board the Mars Express spacecraft. Joint observations have shown that events of intense ionospheric electron density enhancements occur in the lower ionosphere of magnetic cusp regions, and that these enhancements are not associated with precipitation of charged particles above a few hundred electron volts (<300 eV). To account for the enhancement by particle precipitation, electron fluxes are required with mean energy between 1 and 10 keV. No ionizing radiation, neither energetic particles nor X-rays, could be identified, which could produce the observed density enhancement only in the spatially limited cusp regions. Actually, no increase in ionizing radiation, localized or not, was observed during these events. It is argued that the process causing the increase in density is controlled mainly by convection of ionosphere plasma driven by the interaction between the solar wind and crustal magnetic field lines leading to excitation of two-stream plasma waves in the cusp ionosphere. The result is to heat the plasma, reduce the electron–ion recombination coefficient and thereby increase the equilibrium electron density.

Keywords: Mars; Ionosphere; Convection; Sounding radar

1. Introduction

The topside radio wave sounder MARSIS (Mars Advanced Radar for Subsurface and Ionosphere Sounding) (Picardi et al., 2004) on board the Mars Express spacecraft (Chicarro et al., 2004) measures reflections from electron densities in the Martian ionosphere as a function of frequency and radio wave propagation time (Gurnett et al., 2005). Several different kinds of targets giving rise to reflections have been identified, and a variety of them are poorly understood. Single and double peaks in the vertical profile of electron density have been observed, oblique echoes from upward bulging ionosphere in cusp regions (see Duru et al. (2006); Nielsen et al. (2007)), diffuse echoes from off-nadir directions, and possible holes in the ionosphere are indicated. The most common observation is vertical reflections from nadir. Electron densities in the Martian ionosphere are generally horizontally stratified and the dominating observation by the sounder is vertical reflections from these layers. Techniques have been developed whereby the observations are inverted to the vertical profile of electron densities (Nielsen et al., 2006). The primary density peak in the profile conforms to the predictions of photochemical equilibrium between ionization and recombination in a plasma. For example, the peak

*Corresponding author. Tel.: +49 5556 979450.
E-mail address: nielsen@mps.mpg.de (E. Nielsen).

0032-0633/$ - see front matter © 2007 Elsevier Ltd. All rights reserved.
doi:10.1016/j.pss.2007.07.003

density conforms to a predicted spatial variation controlled by the solar zenith angle (Chapman, 1931; Gurnett et al., 2005; Nielsen et al., 2006). However, at times sudden short lasting strong increases are observed in the maximum electron density in the primary density peak. This separates the events from the overall behavior of the background ionosphere observed along the spacecraft trajectory. Such intense events have been mentioned before (Gurnett et al., 2007) and are analyzed in this work invoking charged particle measurements by the particle detector ASPERA-3 (Analyzer of Space Plasmas and Energetic Atoms-3) on board Mars Express (Barabash et al., 2006; Lundin et al., 2004). An absence of extra ionizing radiation during these events points to local processes in the ionosphere as the cause for the increase in electron density.

2. Observations

During ionosphere soundings with MARSIS echoes are observed for a series of discrete frequencies (160). The sweep through frequencies last ~1.2 s and the measurements are repeated with ~7.5 s intervals. The maximum signal frequency for which an echo is recorded (before the radar signal passes through the ionosphere without reflection) is here taken as a measure of the peak plasma frequency (~electron density) in the ionosphere primary layer. In Fig. 1, observations during three different orbits are displayed in three vertical stacks of panels. The top panel in each stack is the peak density versus Universal Time. During each orbit there is a component of the maximum density slowly varying with time along the trajectory. This slow variation is occasionally interrupted by short lasting strong increases of the density. Electron density enhancement occurred during one time interval of orbit #2304, on October 29, 2005. In both orbits #2359 from November 14, 2005, and #2491 from December 21, 2005, there are three intervals with strong deviations. The mean increase in the excursions is on average about 50% over background. The altitude of the peak density in the excursions is <125 km. The time duration of the strong

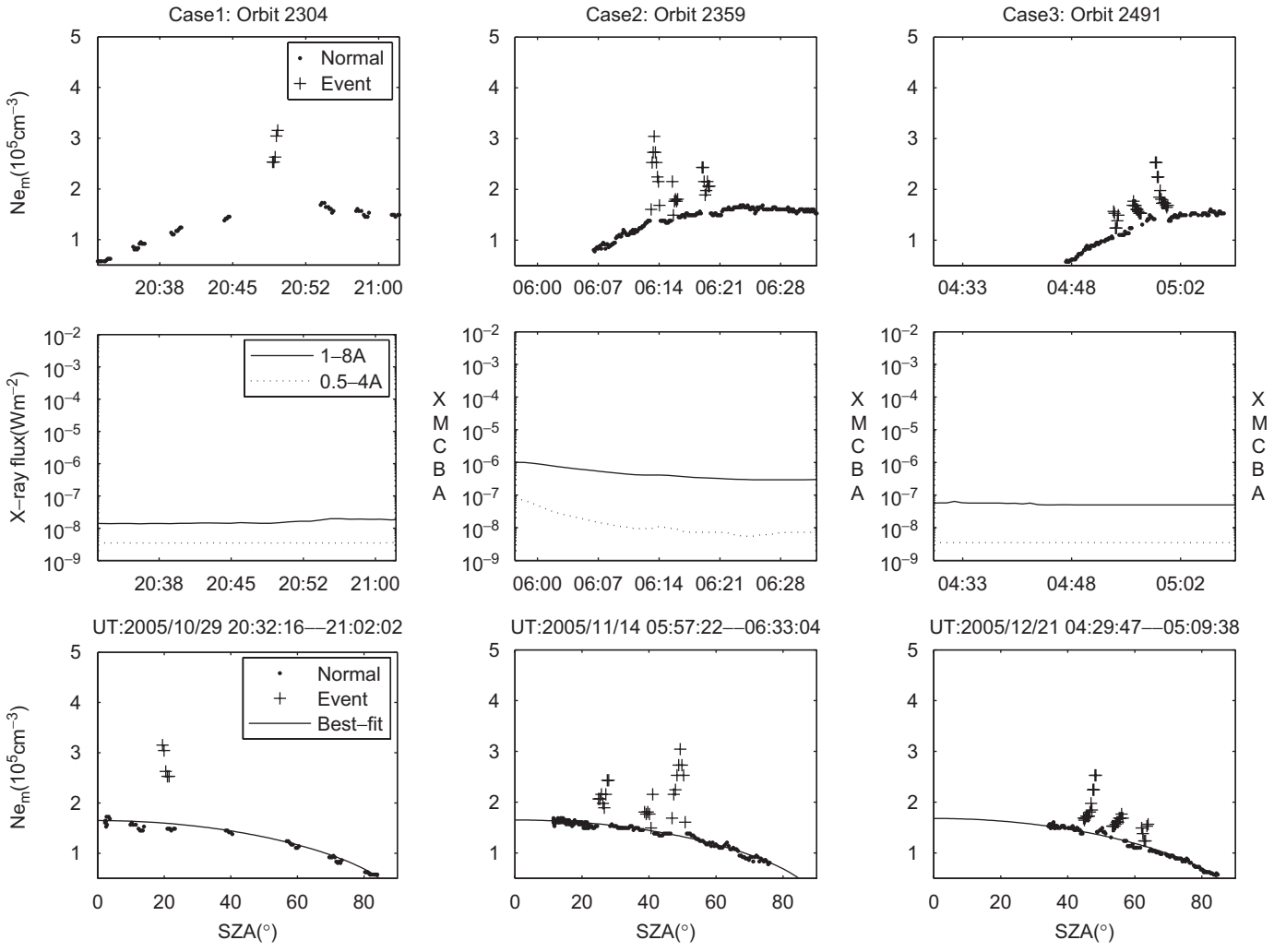

Fig. 1. Strong peak electron density enhancement events observed during three orbits. The maximum density shown as function of Universal Time (top panels) and solar zenith angle (lower panels). X-ray flux at GOES versus time showing absence of solar activity during the observations (center panels).

increases was less than 1 min. During these measurements the spacecraft was at low altitudes near 300 km where the spacecraft is moving rapidly with a speed of ~5 km/s.

An event lasting a short time when observed from a moving spacecraft can be either an impulsive event in time or indicate a small-scale spatial structure rapidly crossed by the spacecraft. It has been shown before that impulsive solar X-ray bursts are causing sudden increases in the Martian electron densities (Mendillo et al., 2006; Nielsen et al., 2006). In the middle panels of Fig. 1 the solar X-ray flux from 1 to 8 Å observed on the GOES (Geostationary Operational Environmental Satellite) spacecraft are shown for the times of MARSIS events (Bornmann et al., 1996). Clearly, no solar X-ray activity was detected during these times. Solar cosmic rays are also known to influence the ionosphere densities (Morgan et al., 2006). Examination of charged particle fluxes observations on board ACE (Advanced Composition Spacecraft) and on board SOHO (SOlar and Heliospheric Observatory) during the times of the events, revealed no enhanced energetic charged particle activity. GOES, SOHO and ACE are located near the Earth, which was separated from Mars by an azimuth angle of 29.4° (#2491), 6.2° (#2359), and 7.9° (#2304) (with the orbit number in parenthesis). Neither at the time of the events, nor when taking into account co-rotation time and radial distance differences from the Earth to Mars, could large-scale sporadic energetic precipitation be found to account for the measurements. It follows that the events are more likely associated with spatially limited processes.

In the lowest panels in Fig. 1 the peak densities are shown as function of solar zenith angle. The background densities are smoothly varying and well-fitted by a curve reflecting the theoretical variation of the peak density versus zenith angle in a Chapman layer. The events are observed between 20° and 60° zenith angle, i.e. well into the dayside ionosphere. The duration of the events and the speed of the spacecraft combines to indicate that the spatial scale of the enhancements was <300 km. This corresponds to about 5° in latitude. The only structures on Mars, which may have effects in the ionosphere with such a scale, are the crustal magnetic fields. Crustal magnetic fields on Mars were observed by MGS (Mars Global Surveyor); they maximize in the southern hemisphere in the region bounded by 130–250° in east longitude and −85° to −10° latitude (Acuna et al., 1998, 1999; Connerney et al., 1999). Magnetic field measurements in 400 ± 30 km (Connerney et al., 2001) were used to determine the global variations of magnetic field inclination and magnitude. The result in the region of strong fields is shown in Fig. 2. The top panel in Fig. 2 shows the magnetic inclination. 'Blue' color is upward-pointing vertical field, and 'red' demarks downward-pointing fields. There is a strong spatial variation, especially in latitude, with oppositely directed fields alternating with each other, separated by regions of closed magnetic field lines ('green'). In the lower panel, the magnitude of the magnetic field shows a single strong maximum. Superposed on this are the ground tracks for the three orbits under investigation, with the locations marked at which events with strong density enhancement were observed. It reveals a clear pattern in which the events occur in magnetic cusp regions with vertical magnetic field lines (with upward- or downward-pointing magnetic fields). Further, the events were observed in the region of strongest crustal magnetic fields.

With the location of enhanced densities limited to the cusp regions, local acceleration of charged particles somewhere along the magnetic field lines may be a possible cause of the density increase (Lundin et al., 2004). Fortunately, the ASPERA-3 particle experiment was in operation during these events. The ASPERA-3 instrument is described in Barabash et al. (2006). The instrument consists of an electron spectrometer (ELS), an ion spectrometer (IMA) and three neutral particle sensors. Fig. 3 (top panel) shows a spectrogram from the ELS observed during orbit #2359. The energy range of the sensor is 0.4–20 keV, but at this time, electrons with energies below 5 eV are reflected to avoid saturation of the counters. Shown are counts obtained during 4 s sampling intervals by all 16 anodes of the sensor. After 0629 UT, the spacecraft enters the magnetosheath, and before that the spacecraft is inside the photoelectron boundary. We observe that there are no significant fluxes of electrons above 300 eV. Specifically, no energetic electron flux coincided with the ionosphere electron density increases observed by MARSIS (Fig. 1). The ELS sensor can roughly estimate electron bulk velocities using 16 anodes mounted in a plane. This estimate indicates radially outward flows for all flux enhancements. The IMA sensor observes no ions with energies above 300 eV; specifically no protons. For periods of less than 12 s, heavy ion flows with energies of less than 200 eV/charge are observed. The flow speed of these ions is lower than 10 km/s and directed outward. The middle panel shows similar electron data for orbit #2491. Also, for this orbit there are no electrons above 300 eV and only low-energy ions associated with the electron flux increases at 10–300 eV. The bulk velocities were directed outward. The crucial observation in our context is that there were no energetic electron or ion fluxes observed during the entire time interval including the time when electron density enhancements were observed in the lower ionosphere. Furthermore, the bulk velocity of the observed electrons and ions were directed outward, i.e. there was no precipitation of higher energy charged particles into the ionosphere. The spatial locations, where these excursions of electron fluxes into higher energies up to 300 eV occurred, are shown in the lower panel on top of a map of crustal magnetic field inclination. The spatial locations, where the more energetic electrons were observed, are only marked where the magnetic field magnitude is large (>100 nT; so as to minimize solar wind effects) and the spacecraft altitude is below 500 km (near the altitude for the Connerney-model magnetic fields). The low-energy electron fluxes tend to be located in the cusp regions. However, the correlation is not as clear as for the density

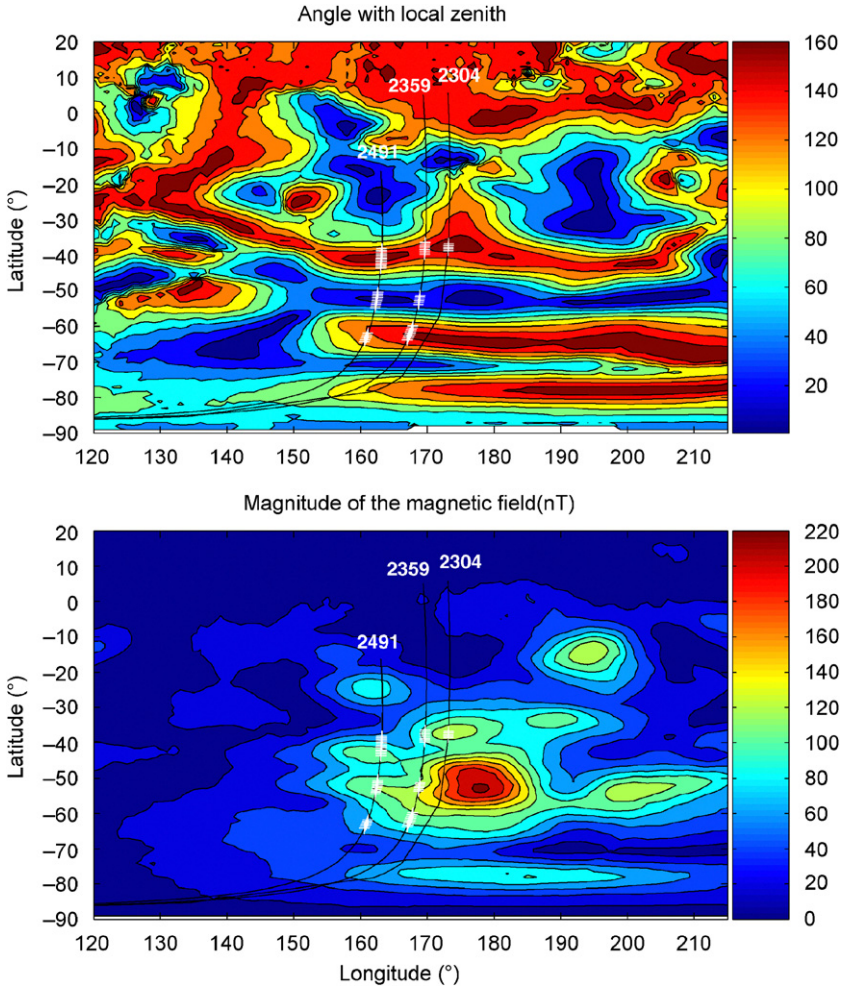

Fig. 2. Spatial maps of the inclination (top panel) and magnitude (lower panel) of the Martian crustal magnetic fields (Connerney et al., 2001). Superposed on both maps are the ground tracks of the relevant orbits with locations marked where peak density enhancements were observed. There is a clear relation of the enhanced density events with vertical magnetic field and with the magnitude of the field.

enhancements. This indicates that low-energy electron fluxes tend to be more smeared out across the magnetic field. The exact spatial coincidence of 300 eV electrons and cusp regions remains tentative. The main reason for this 'smearing' may be that the spatial variations of the crustal magnetic field is modified during these events (occurring on the dayside) by a magnetic field component induced from the interaction of the solar wind with the ionosphere. This would directly influence the spatial distribution of the low energy electrons.

Detrick et al. (1997) determined the minimum altitude an electron can penetrate into the Martian atmosphere before being stopped. With peak density enhancement located below 125 km, precipitating electrons with energies >1 keV are required. Thus, no energetic charged particle precipitation was observed, which could possibly account for the increase of the density maximum. The near-vertical magnetic field lines that connect to the nadir region where the sounder measurements were made, did not carry any energetic particles which could conceivably increase the ionization rate in the lower ionosphere to the point of accounting for the observed density enhancement.

Fig. 4 shows two MARSIS spectrograms taken on November 14, 2005 (orbit #2359): panel 'a' shows the observed echoes outside the cusp regions and panel 'b', observations in the cusp. The outstanding difference between observations in the two magnetically different regions is the increase of the maximum frequency in the cusp: from 3.2 to ~5 MHz; an increase of a factor 1.5. This is one of the largest increases observed and corresponds to an increase in the maximum electron density by a factor ~2.2. The mean value of the density increase (Fig. 1) is close to a factor 1.5. The observations are inverted to yield the vertical electron density profiles following the procedure outlined in Nielsen et al. (2006). The result is shown in Fig. 5. The solid curves (marked 141 and 132, respectively) are the inverted profiles corresponding to the data in the left-hand and right-hand panels in Fig. 4. The two dashed curves are Chapman layer fits to the density profiles around the density maximum, and the dotted

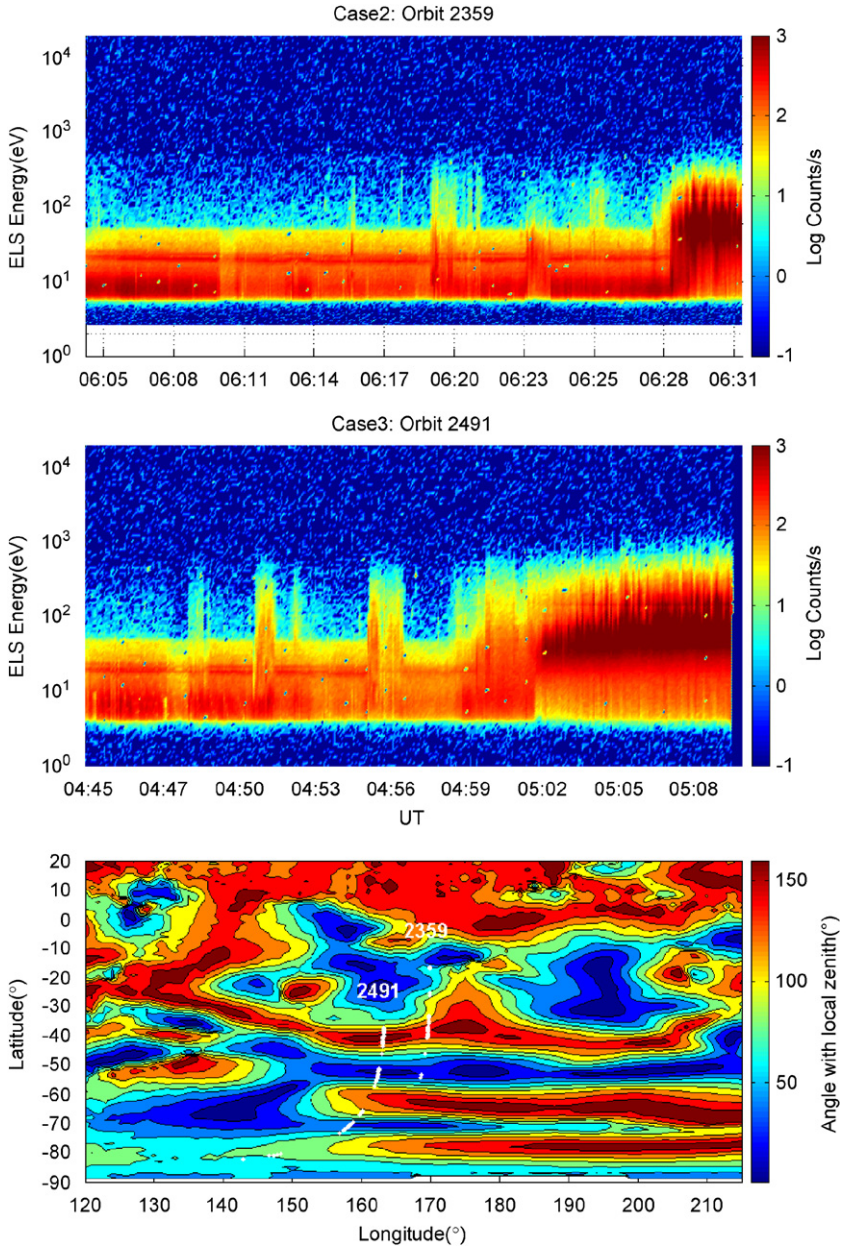

Fig. 3. ASPERA-3 electron flux observations during two of the relevant orbits are in the two upper panels. Note the occasional flux enhancements of electron energies <300 eV. The locations of flux enhancements are plotted on the map of magnetic inclination shown in the lower panel. The enhancements tend to occur in cusp regions of vertical crustal magnetic fields coinciding with enhanced densities.

curve is the difference between the cusp and outside-cups profiles. The largest density increase for this event was near the peak altitude of 110 km.

3. Discussion

The density profile around the density peak is determined by photochemical equilibrium between ionizing radiation and recombination of electrons and ions. In an equilibrium situation, the electron density is proportional to the square root of the ratio of electron–ion production (by ionizing radiation) and ion–electron recombination coefficient.

One way to increase the equilibrium density would be to enhance the intensity of the ionizing radiation keeping everything else constant. However, no enhancement of solar activity in the form of solar energetic radiation or precipitation of solar cosmic rays occurred, and no local accelerations of charged particles were observed which could produce the enhanced densities. The particle detector observed only an increase in the very low energy electron flux directed away from the planet. Thus, neither large-scale 'global' nor small-scale 'local' enhanced precipitation of

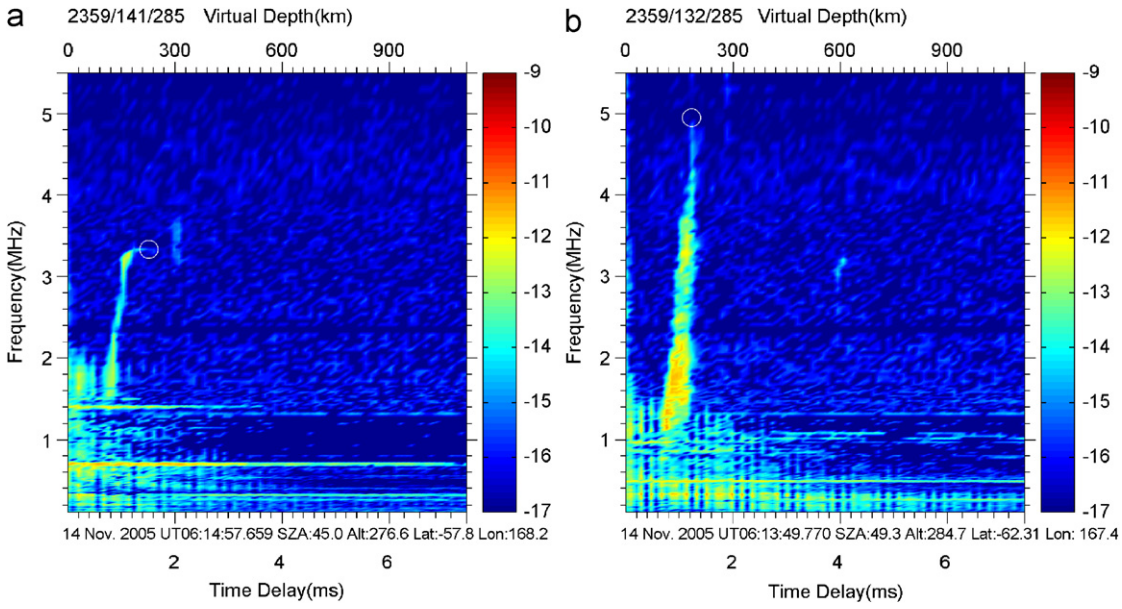

Fig. 4. Spectrograms of MARSIS observations outside (panel a) and inside (panel b) a cusp region. Note the increase of the largest reflected frequency (~maximum peak density) on entering the cusp.

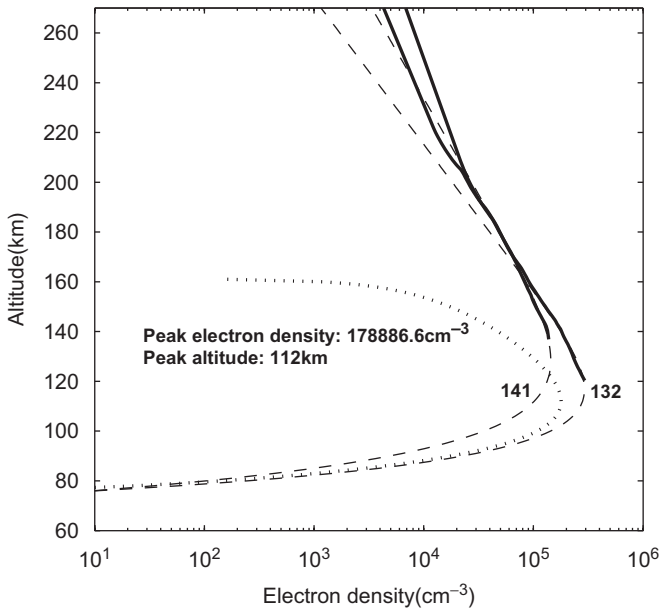

Fig. 5. Vertical electron density profiles corresponding to the observations shown in Fig. 4. The dashed curves are fits of a Chapman function to the low-altitude measurements. The dotted curve is the difference between the two density profiles and represents the enhancement of electron densities in the cusp region.

energy into the Martian ionosphere can account for the events. The ionization production term appears to be constant.

Another possibility for enhanced electron density is a reduction of the recombination coefficient α. A doubling of the equilibrium density would require a fourfold decrease of the recombination coefficient. The dominant ion at the altitudes near the density maximum is O_2^+. For electron temperatures below 1200 K, the dissociative recombination rate for that ion is $\alpha = 1{\cdot}9 \times 10^{-7}(300/T_e)^{0{\cdot}7}$ (Schunk and Nagy, 2000)· Thus, an increase of the density by a factor between 1.5 and 2 implies an increase of the electron temperature by a factor between 3.2 and 7.2. If the electron temperature outside the cusp was 200 K, then in the cusp ionosphere it would have to increase to between 600 and 1500 K. This considerable heating does not come from energetic precipitation from the Sun or from acceleration processes along the magnetic field lines, but must be produced by local plasma processes.

In the Earth's ionosphere, considerable heating of the electron gas by plasma wave activity is a well-known phenomenon (Dimant and Milikh, 2003; St.-Maurice, 1990; St.-Maurice et al., 1990). Charged particle motion in the ionosphere is basically governed by an imposed electric field (E), by gyro motion in a magnetic field (B) and by collisions with other particles. Above ~130 km in the Earth's ionosphere, both electrons and ions are $E \times B$ drifting, suffering few collisions. Below ~80 km, the motion of both species are controlled by collisions. In the altitude range from 80 to 130 km, electrons are $E \times B$ drifting while ion motion is controlled by collisions. When the relative bulk speed of electrons and ions exceeds the ion acoustic velocity, plasma waves appear as the two-stream instability is excited (or Farley–Buneman plasma instability; Fejer and Kelly, 1981). In the auroral zone, where strong convection electric fields often occur, the relative electron–ion speed and electron density peak maximize in the E-region, where the ion acoustic velocity is about 400 m/s. Typically, plasma waves are observed when the ionospheric electric field exceeds 20 mV/m (corresponding to an $E \times B$ speed of ~400 m/s) when electrons are driven with supersonic speed through the collision-dominated

ions. Radar observations have demonstrated strong enhancements of electron temperature in the E-region during strong electric field events. It was concluded that the temperature of the electron gas is enhanced when the convection electric field is strong enough to drive the electrons through the ion gas at supersonic speed. St.-Maurice et al. (1981) reported increases of electron temperatures from 300 to 1500 K. The conventional frictional (Joule) heating caused by the DC electric field cannot account for the observed high electron temperatures. It is now generally accepted that the strong electron temperature increase is anomalous and caused by the turbulent electric fields in Farley–Buneman plasma waves. That enhanced electron temperatures are associated with excitation of the two-stream instability is well documented (Foster and Erickson, 2000; Nielsen and Schlegel, 1985). Nielsen and Schlegel (1985) examined the relationship between coherent phase velocity measurements in the E-region with electron drift velocities in the F-region (~electric field) and found the phase velocity to be limited to a value near the ion acoustic velocity. They also found this limiting phase velocity to be a strongly increasing function of the electric field. This increase of the ion acoustic velocity with electric field magnitude was interpreted as heating of the E-region electron gas by the unstable two-stream plasma waves. Robinson (1986) has shown that there is an ample source of energy in unstable waves resulting from excitation of the two-stream instability, and found that the anomalous electron temperatures in the disturbed high latitude E-region can be quantitatively explained in terms of heating by plasma waves. The predicted variation of ion acoustic velocity and electric field showed a weak dependence on DC Joule heating but a strong dependence on heating of the gas by unstable waves. Sudan et al. (1973) proposed to describe the anomalous heating of the electron gas by replacing the electron-neutral collision frequency with an anomalous collision frequency. Nielsen (1986) found the anomalous frequency to be a factor between 4 and 6 larger than the normal frequency. Since plasma heating is proportional to the collision frequency, this increase is associated with strongly enhanced heating.

Heating of the electron gas leads to a decrease of the recombination coefficient and an increase of the electron density. While the heating is well established, the density increase is less well established. But recently, Milikh et al. (2006) reported electron density and temperature observations in the Earth's high latitude ionosphere during heating events. They found anomalous electron heating to be localized between 100 and 120 km, where the magnetized electron bulk speed exceeds the acoustic speed of the unmagnetized ions leading to the Farley–Buneman instability. Because the electric fields were strong (>100 mV/m, corresponding to >2000 m/s $E\times B$ drift speed) the instability resulted in strong anomalous heating. Heating from a background electron temperature of 500 K up to 2500 K was observed. The associated enhancements in the electron density were observed to be up to a factor 2, or near a doubling of the electron density between 100 and 120 km. The electron density perturbations showed a good agreement with the model that accounts for suppression of the electron/ion recombination rate due to anomalous electron heating.

The conditions for particle motion and excitation of the two-stream instability near the primary electron density peak in the Martian ionosphere are quite similar to the conditions in the Earth's E-region. For a magnetic field amplitude of 1000 nT, the electron gyro frequency is 28.4 kHz, which equals the electron collision frequency in ~90 km altitude. Thus, electrons are magnetized above 90 km height. Similarly, the ions are unmagnetized below an altitude of ~150 km where the gyro frequency of the dominating ion and its collision frequency have the same magnitude (~0.5 Hz). In this altitude range, there is a relative motion between electrons and ions. For a sufficiently large electric field the speed of the electrons will exceed the ion acoustic speed and excite the two-stream instability resulting in heating of the electron gas.

The driving force in this scenario is the electric field. It is suggested that the electric field arises owing to the flow of the solar wind plasma past the crustal magnetic field cusp structures. The magnetic field lines in the cusps extend into the solar wind, and the flow of a conducting medium over the field lines induces an electric field, such that the magnetic field is frozen into the plasma and carried along by plasma motion. The density enhancement events were observed in cusp regions located near the largest crustal magnetic fields on Mars. These strong magnetic fields can reach further into the solar wind than field lines from other regions, an indication that the solar wind interaction with the crustal fields plays a role in forming the events. For a solar wind speed of 200 km/s and a magnetic field magnitude of 1 nT, the induced electric field in the solar wind is $200\times1000\times10^{-9}\times1000\,\mathrm{mV/m}=0.2\,\mathrm{mV/m}$.

Assuming the magnetic field lines are electric equipotentials, the electric field in the ionosphere is increased owing to convergence of the field lines with decreasing altitude: assume an increase of a factor 20–4 mV/m. Let the ionosphere magnetic field be ~500 nT and the $E\times B$ drift speed of the electrons is then $4\times10^{-3}/(5\times10^{-7})\,\mathrm{m/s}=8000\,\mathrm{m/s}$. The ion acoustic velocity in an O_2^+ ion gas with $T_i\sim T_e\sim200$ K is ~450 m/s. The electron speed exceeds the ion acoustic velocity by a large factor. Thus, excitation of the two-stream plasma instability in the Martian ionosphere is a realistic possibility.

Heating of the electron gas is controlled by the electric field magnitude and by the Pedersen conductivity, which is mainly determined by the electron density and the collision frequency (Withers et al., 2005). The electron density typically peaks at altitudes between 90 and 150 km in a region where the electrons are magnetized and the ions unmagnetized. There is a DC component from the applied electric field and an AC component from the turbulent wave electric field. The DC energy deposit in the ionosphere is partly controlled by the

DC electric field and the height integrated Pedersen conductivity, $\Sigma \sim 2 \times N \times e \times H/B$. For a density of $N \sim 2 \times 10^5$ el/cm^3, a scale height $H \sim 12$ km and a magnetic field as above, we find the conductivity to be 1540 S. For a 4 mV/m electric field, the heating is ~ 25 mW/m^2. This is compatible with typical values for the Earth high latitude ionosphere; with $\Sigma \sim 10$ S and $E \sim 50$ mV/m, the heating is ~ 25 mW/m^2. Even though the electric field we have inferred for Mars is small compared to the fields in the Earth's high latitude ionosphere, the DC Joule heating at Mars is compatible to the heating in the Earth ionosphere. The reason for this is the large (height integrated) Pedersen conductivity, or equivalently the large electron-neutral collision frequency in the Martian CO_2 atmosphere; the frequency is ~100 times larger than in the Earth's nitrogen atmosphere. However, at the Earth (and presumably at Mars) this conventional frictional heating cannot account for the electron heating. The increase in electron temperature is widely accepted to be caused by the turbulent (AC) electric field generated by the two-stream plasma instability. The influence of the turbulent electric fields is to increase the effective electron collision frequency by a factor of 4–6. Since the Pedersen conductivity is proportional to the collision frequency, we also expect the wave heating to increase by such a factor 5 to further raise the electron temperature.

It appears that the cusp ionosphere with a solar wind imposed electric field of a few mV/m is unstable to the two-stream instability. Owing to the large collision frequency of electrons with a neutral CO_2 gas, even a modest electric field imposed by the solar wind can cause heating comparable to heating at the Earth, where the Pedersen conductivity is smaller but the electric field is stronger. The Pedersen conductivity is proportional to the electron collision frequency which is increased to an anomalous level by the turbulent wave electric fields. This may result in energy deposits of the order of 100 mW/m^2 and result in enhancement of the electron gas temperature.

If the temperature enhancement is taken to be proportional to the energy deposition, then the density is expected to increase by a factor between 1.6 and 1.9 (for an energy deposit of a factor 5 larger than the DC deposit, the recombination coefficient decreases by a factor $5^{0.7}$ and the density increases by $(5^{0.7})^{1/2} = 1.7$). It is realistic to expect density enhancements by a factor up to 1.5–2.0. If the electron gas temperature changes suddenly from T_0 to T_1, it will take some time for the densities to change to the corresponding equilibrium values. Milikh et al. (2006) determined the time constant to be $\tau = 1/(2 \times (\alpha_1 \times \alpha_o)^{1/2} N_o)$. For a five-fold temperature increase and an initial electron density of 10^5 el/cm^3 we find $\tau = 44$ s. Thus, within a few minutes the system has reached more than 90% of its equilibrium value.

To suggest that heating of a plasma in a flux tube leads to a density increase may seem counter-intuitive. To preserve pressure balance, one would expect the heating to be associated with an (upward) expansion of the heated plasma. This is actually what ASPERA-3 observed. We suggest the upwelling is inhibited and limited by ion-neutral collisions. This may reduce the upwelling so effectively as to lead to an increased density. A condition for the density increase is that the recombination coefficient is strong enough that it overwhelms the upwelling process. A simulation of the heated plasma in a flux tube is planed to check this model.

The predicted quite high electron drift velocities in the ionosphere may give rise to ionization effects if they exceed the Critical Ionization Velocity (CIV), i.e. if the electron kinetic energy, $0.5 \times m_e \times v_{CIV}^2$, exceeds the CO_2 ionization energy of ~35 eV. However, in this case the CIV is much larger ($> 3.6 \times 10^6$ m/s) than realistic drift speeds. The magnetized ions do not take part in this process.

In magnetic cusp regions where crustal magnetic field lines extend far into the solar wind, it appears that an electric field is induced so that the magnetic field lines are carried along with ('frozen into') the plasma. Mapping of the induced convection electric field along equipotential magnetic field lines results in an electric field of a few mV/m impressed on the ionosphere. An electric field of such strength is sufficient to drive electrons through the collisional ions at supersonic speed in the altitude range from 90 to 150 km. This results in excitation of the two-stream instability at those altitudes. With reference to observations in the Earth's ionosphere, where similar conditions typically occur in the E-region, it is suggested that the turbulent electric fields in the two-stream plasma waves heat the electron gas significantly. Recent observations have shown that simultaneous to the temperature enhancement an increase of the electron density in the E-region occurred, which can be understood as a result of lowering of the electron–ion recombination coefficient owing to the temperature increase. It is argued that conditions in the Martian crustal magnetic cusp regions allow similar processes to take place there, to produce the electron density enhancements observed with MARSIS.

Acknowledgments

MARSIS was built and is jointly managed by the Italian Space Agency and NASA. Mars Express was built and is operated by the European Space Agency. The research at the University of Iowa was supported by NASA through contract 1224107 with the Jet Propulsion Laboratory. We thank all members of the ASPERA-3 team for the big effort which led to the successful operation of the instrument and the calibration of the data. For this paper, we are especially grateful to Emmanuel Penou and Andrei Fedorov at CESR for data preparation and IMA calibration and Andrew Coates at MSSL for calibration of the ELS sensor data. We wish to acknowledge support from German DLR grant 50QM99035, and NASA contract NASW-00003 at SWRI. We thank the referees for constructive comments.

References

Acuna, M.H., Connerney, J.E.P., Wasilevsky, P., Lin, R.P., Anderson, K.A., Carlson, C.W., McFadden, J., 1998. Magnetic fields and plasma observations on Mars: initial results on Mars Global Surveyor mission. Science 279, 1676–1680.

Acuna, M.H., Connerney, J.E.P., Ness, N.F., Lin, R.P., Mitchell, D., et al., 1999. Global distribution of crustal magnetization discovered by the Mars global Surveyor MAG/ER experiment. Science 284, 790.

Barabash, S., Lundin, R., et al., 2006. The analyzer of space plasmas and energetic atoms (ASPERA-3) for the Mars Express mission. Space Sci. Rev. doi:10.1007/s11214-006-9124-8.

Bornmann, P.L., Speich, D., Hirman, J., Mathison, L., Grubb, R., Garcia, H., Viereck, R., 1996. GOES X-ray sensor and its use in predicting solar-terrestrial distances. Proc. SPIE 2812, 291.

Chapman, S., 1931. The production of ionization by monochromatic radiation incident upon a rotating atmosphere, Part II. Grazing incidence. Proc. Phys. Soc. 43, 483.

Chicarro, A., Martin, P., Traunter, R., 2004. The Mars Express mission: an overview. In: Wilson, A. (Ed.), Mars Express: A European Mission to The Red Planet, SP-1240. European Space Agency Publication Division, Noordwijk, the Netherlands, pp. 3–16.

Connerney, J.E., Acuna, M., Wasilewski, P., Ness, N., Reme, H., Mazelle, C., Vignes, D., Lin, R., Mitchell, D., Cloutier, P., 1999. Magnetic lineations in the ancient crust of Mars. Science 284, 794.

Connerney, J.E., Acuna, M.H., Wasilewski, P.J., Kletetschka, G., Ness, N.F., Reme, H., Lin, R.P., Mitchell, D.L., 2001. The global magnetic field of Mars and implications for crustal evolution. Geophys. Res. Lett. 28 (21), 4015.

Detrick, D.L., Rosenberg, T.J., Fry, C.D., 1997. Analysis of the Martian atmosphere for riometry. Planet. Space Sci. 45 (3), 289.

Dimant, Y.S., Milikh, G.M., 2003. Model of anomalous electron heating in the E region: 1. Basic theory. J. Geophys. Res. 108 (A9), 1350.

Duru, F., Gurnett, D.A., Averkamp, T.F., Kirchner, D.L., Huff, R.L., Persoon, A.M., Plaut, J.J., Picardi, G., 2006. Magnetically controlled structures in the ionosphere of Mars. J. Geophys. Res. 111, A12204.

Fejer, B.G., Kelly, M.C., 1981. Ionosphere irregularities. Rev. Geophys. 18, 401.

Foster, J.C., Erickson, P.J., 2000. Simultaneous observations of E-region coherent backscatter and electric field amplitude at F-region heights with the Millstone Hill UHF radar. Geophys. Res. Lett. 27(19), 3177, 2000GL000042.

Gurnett, D.A., Kirchner, D.L., Huff, R.L., Morgan, D.D., Persoon, A.M., Averkamp, T.F., Duru, F., Nielsen, E., Safaeinili, A., Plaut, J.J., Picardi, G., 2005. Radar soundings of the ionosphere of Mars. Science 310, 1929.

Gurnett, D.A., Huff, R.L., Morgan, D.D., Persoon, A.M., Averkamp, T.F., Kirchner, D.L., Duru, F., Akalin, F., Kopf, A.J., Nielsen, E., Safaeinili, A., Plaut, J.J., Picardi, G., 2007. An overview of radar soundings of the Martian ionosphere from the Mars Express spacecraft. Adv. Space Research, in press, 2007.

Lundin, R., et al., 2004. Solar wind-induced atmospheric erosion at Mars: first results from ASPERA-3 on Mars Express. Science 305, 1933–1936.

Mendillo, M., Withers, P., Hinson, D., Risbeth, H., Reinisch, B., 2006. Effects of solar flares on the ionosphere of Mars. Science 311, 1135.

Milikh, G.M., Goncharenko, L.P., Dimant, Y.S., Thayer, J.P., McCready, M.A., 2006. Anomalous electron heating and its effects on the electron density in the auroral electrojet. Geophys. Res. Lett. 33, L13809, doi:10.1029/2006GL026530.

Morgan, D.D., Gurnett, D.A., Kirchner, D.L., Huff, R.L., Brain, D.A., Boynton, W.V., Acuña, M.H., Plaut, J.J., Picardi, G., 2006. Solar control of radar wave absorption by the Martian ionosphere. Geophys. Res. Lett. 33, L13202, doi:10.1029/2006GL026637 (J13).

Nielsen, E., 1986. Aspect angle dependence of mean Doppler velocities of 1-m auroral plasma waves. J. Geophys. Res. 91, 10173.

Nielsen, E., Schlegel, K., 1985. Coherent radar Doppler measurements and their relationship to the ionospheric electron drift velocity. J. Geophys. Res. 90, 3498.

Nielsen, E., Wang, X.D., Gurnett, D.A., Kirchner, D.L., Huff, R.L., Orosei, R., Safaeinili, A., Plaut, J.J., Picardi, G., 2007. Vertical sheets of dense plasma in the topside Martian ionosphere. J. Geophys. Res., in press, 112, E02003, doi:10.1029/2006je002723.

Nielsen, E., Zou, H., Gurnett, D.A., Kirchner, D.L., Morgan, D.D., Huff, R.L., Orosei, R., Safaeinili, A., Plaut, J.J., Picardi, G., 2006. Observations of vertical reflections from the topside Martian ionosphere. Space Sci. Rev., doi:10.1007/s11214-006-9113-y.

Picardi, G., Biccari, D., Seu, R., et al., 2004. MARSIS: Mars advanced radar for subsurface and ionosphere sounding. In: Wilson, A. (Ed.), Mars Express: A European Mission to The Red Planet, SP-1240. European Space Agency Publication Division, Noordwijk, the Netherlands, pp. 51–70.

Robinson, T.R., 1986. Towards a self-consistent non-linear theory of radar auroral backscatter. J. Atmos. Terr. Phys. 48, 417.

Schunk, Nagy, 2000. Ionospheres. Cambridge University Press, New York.

St.-Maurice, 1990. Electron heating by plasma waves in the high latitude E-region and related effects: observations. Adv. Space Res. 10 (6), 239.

St.-Maurice, J.P., Schlegel, K., Banks, P.M., 1981. Anomalous heating of the polar E region by unstable plasma waves. II–Theory. J. Geophys. Res. 86, 1453.

St.-Maurice, Kofman, W., kluzek, E., 1990. Electron heating by plasma waves in the high latitude E-region and related effects: observations. Adv. Space Res. 10 (6), 225.

Sudan, R.N., Akinrimisi, J., Farley, D.T., 1973. Generation of small scale irregularities in the equatorial electrojet. J. Geophys. Res. 78, 240.

Withers, P., Mendillo, M., Risbeth, H., Hinson, D.P., Arkani-Hamed, J., 2005. Ionospheric characteristics above Martian crustal magnetic anomalies. Geophys. Res. Lett. 32, L16204, doi:10.1029/2005GL023483.